

INTERLEAVED BOOST CONVERTER WITH MPPT TECHNIQUE FOR PHOTOVOLTAIC SYSTEM

Ajeet Kumar Singh¹, Upasana Singh²

¹PG Scholar, Department of Electrical Engineering,

College of Technology and Engineering, Udaipur, Rajasthan, (India)

²UG Scholar, Institute of Engineering and Technology, Sitapur, U.P. (India)

ABSTRACT

Interleaved boost converters consists of several identical boost converters connected in parallel and controlled by interleaving technique which has the same switching frequency and phase shift. Increased efficiency, reduced size and improved reliability are major advantages of interleaved boost converter.

Keywords – Interleaved Boost Converter, Ripple Minimization, MPPT, Coupling

I INTRODUCTION

Energy sources with low output voltage such as fuel cell stacks and photo-voltaic (PV) generation system attracts many researchers because they appear to be the possible solutions to the environmental problems.

DC – DC converters are important component as power electronics interfaces for photovoltaic generators and other renewable energy sources. Interleaved method used to improve power converter performance in terms of efficiency, size, conducted electromagnetic emission, and transient response. The benefits of interleaving include high power capability, modularity, and improved reliability. However, an interleaved topology improves converter performance at the cost of additional inductors, power switching devices, and output rectifiers.

II INTERLEAVED OPERATION

The interleaved boost converters consists of several identical boost converters connected in parallel and controlled by the interleaved method which has the same switching frequency and phase shift. Ripple cancellation both in the input – output voltage and current waveforms, reduced peak value, and high ripple frequency are some of the benefits of interleaved boost converters. These interleaved boost converters are distinguished similar with conventional converters by critical operation mode, discontinuous conduction mode (DCM), and continuous conduction mode (CCM). In critical mode, filter design is more difficult because critical point vary by load. In the DCM although the disadvantages of reverse recovery effects of boost diodes are improved, there are advantages

such as high input peak current and conduction losses, and lower input peak current. High power applications are easily achieved with CCM.

In Fig.1 after, S_1 turns-on, current increases linearly in L_1 . In this interval energy stored in L_1 . When S_1 turns-off, D_1 conducts the stored energy in L_1 to the load and output capacitor. Current in L_1 down with a slope dependent on the difference between the input and output voltage. After a half period of S_1 switching cycle, S_2 also turns-on, completing the same cycle of events. Since both power channels are combined at the output capacitor, the effective ripple frequency is twice that of a single phase boost converter.

Two phase interleaved boost topology is drawn below.

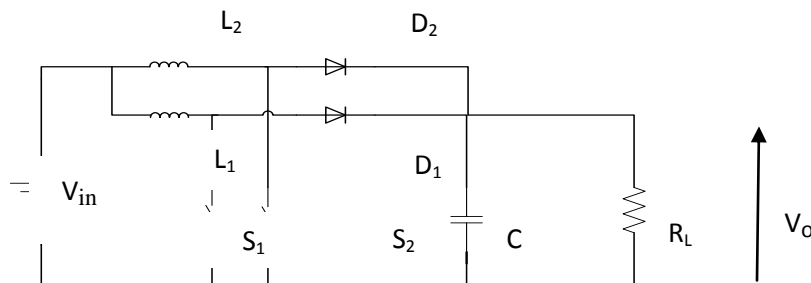


Fig.1

III PV SYSTEM WITH MPPT

In this paper, an analysis of a PV-fed interleaved boost converter (IBC) was carried out. An IBC with two boost converters connected in parallel was considered for this work. The component of the studied system include the PV panel, a boost converter (conventional or IBC), load (R or R-L), maximum power point tracking (MPPT) using an incremental conductance (INC) algorithm and pulse generating circuit. Design, modelling, and simulation of each section in the schematic is discussed below.

IV MATHEMATICAL MODEL OF PV SYSTEM

Mathematical Model of PV System a group of PV cells together form the PV power generation system. The solar system configuration consists of a required number of solar photovoltaic cells, commonly referred to as PV modules, connected in series or in parallel to attain the required voltage output. The basic equation from the theory of semiconductors that mathematically describes the I-V characteristic of the ideal PV cell is

$$I = I_{pv,cell} - I_{0,cell} \left[\exp\left(\frac{qV}{\alpha kT}\right) - 1 \right] \quad \dots\dots (1)$$

The above elementary PV cell does not represent the I-V characteristic of a practical PV array. Cells connected in parallel increase the current and cells connected in series provide greater output voltages.

Practical arrays are composed of several connected PV cells and the observation of the characteristics at the terminals of the PV array requires the inclusion of additional parameters to the basic equation

$$I = I_{pv} - I_0 \left[\exp \left(\frac{V + R_s I}{V_t \alpha} \right) - 1 \right] - \frac{V + R_s I}{R_p} \quad \dots\dots\dots (2)$$

All PV array datasheets bring basically the nominal open-circuit voltage ($V_{oc,n}$), the nominal short-circuit current ($I_{sc,n}$), the voltage at the MPP (V_{mp}), the current at the MPP (I_{mp}), the open-circuit voltage/temperature coefficient (KV), the short circuit current/temperature coefficient (KI), and the maximum experimental peak output power ($P_{max,e}$). This information is always provided with reference to the nominal condition or standard test conditions (STC's) of temperature and solar irradiation. The practical PV device has a series resistance R_s whose influence is stronger when the device operates in the voltage source region and a parallelresistance R_p with stronger influence in the current source region of operation. The assumption $I_{sc} \approx I_{pv}$ is generally used in the modeling of PV devices because in practical devices the series resistance is low and the parallel resistance is high. The diode saturation current is given by

$$I_0 = \frac{I_{sc,n} + K_I \Delta T}{\exp \left(\frac{V_{oc,n} + K_V \Delta T}{\alpha V_t} \right) - 1} \quad \dots\dots\dots (3)$$

The saturation current I_0 is strongly dependent on the temperature so that the net effect of the temperature is the linear variation of the open-circuit voltage according to the practical voltage/temperature coefficient. This equation simplifies the model and cancels the model error at the vicinities of the open-circuit voltages, and consequently, at other regions of the I-V curve

$$I_{pv} = (I_{pv,n} + K_I \Delta T) \frac{G}{G_n} \quad \dots\dots\dots (4)$$

The relation between R_s and R_p , the only unknowns of (2) may be found by making $P_{max,m}=P_{max,e}$ and solving the resulting equation for R_s , as shown

$$P_{max,m} = V_{mp} \left\{ I_{pv} - I_0 \left[\exp \left(\frac{q}{kT} \frac{V_{mp} + R_s I_{mp}}{\alpha N_s} \right) - 1 \right] - \frac{V_{mp} + R_s I_{mp}}{R_p} \right\}$$

$$= P_{max,e}$$

$$R_p = \frac{V_{mp} + I_{mp} R_s}{\left\{ V_{mp} I_{pv} - V_{mp} I_0 \exp \left[\frac{(V_{mp} + I_{mp} R_s) q}{N_s \alpha} \right] + V_{mp} I_0 - P_{max,e} \right\}}$$

find the value of R_s (and hence, R_p) that makes the peak of the mathematical P–V curve coincide with the experimental peak power at the (V_{mp}, I_{mp}) point. This requires several iterations until $P_{max,m} = P_{max,e}$. Each iteration updates R_s and R_p toward the best model solution.

$$I_{pv,n} = \frac{R_p + R_s}{R_p} I_{sc,n}$$

The initial value of R_s may be zero. The initial value of R_p may be given by

$$R_{p,min} = \frac{V_{mp}}{I_{sc,n} - I_{mp}} - \frac{V_{oc,n} - V_{mp}}{I_{mp}}$$

Above equation determines the minimum value of R_p , which is the slope of the line segment between the short-circuit and the maximum-power remarkable points. Although R_p is still unknown, it surely is greater than $R_{p,min}$ and this is a good initial guess.

V MAXIMUM POWER POINT TRACKING

Maximum Power Point Tracking, frequently referred to as MPPT, operates Solar PV modules in a manner that allows the modules to produce all the power they are capable of generating. MPPT algorithms are used to obtain the maximum power from the solar array based on the variation in the irradiation and temperature. Among several techniques, the Perturb and Observe (P&O) method and the Incremental Conductance (InCond) algorithm are the most commonly applied algorithms. Here I am going to explain Incremental Conductance (In Cond) algorithms as

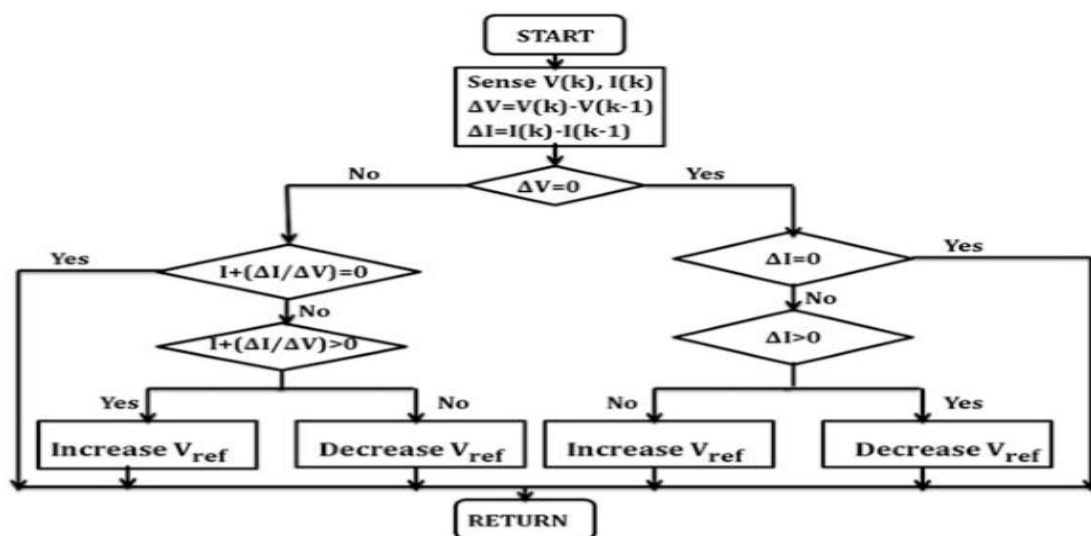


Fig.2 Flow-chart of Incremental Conductance (InCond) algorithm

VI DESIGN AND SIMULATION OF INTERLEAVED BOOST CONVERTER

As the efficiency of Solar PV system is only about 13 to 16% for the silicon mono/poly crystalline types which are commonly used, the power produced by it should be efficiently utilized. To achieve this, converters are used as MPPTs. However, the normal boost converters do not satisfy all requirements, such as low value of ripple in the inductor current in the input side and highly efficient operation even at lower insolation levels. For this purpose, two such boost converters are put in parallel and operated as IBCs. Although IBC overcomes the drawbacks of conventional boost converters, its static and dynamic performances are poor. Hence, a new model consisting of coupled inductors in parallel are used. These coupled inductors reduce the ripple content in the inductor current on the input side by interleaving principles. Boost converter design equations are given as

$$V_s DT = \frac{V_o - V_s}{(1-D)I}$$

As the name of the converter suggests, the output voltage is always greater than the input voltage. The boost converter operates in the CCM for $L > L_b$ where,

$$L_b = \frac{(1-D^2)DR}{2f}$$

The current supplied to the output RC circuit is discontinuous. Thus, a larger filter capacitor is required to limit the output voltage ripple. The filter capacitor C_{min} must provide the output DC current to the load when the diode D is off. The minimum value of the filter capacitance results in the ripple voltage V_r is given by

$$C_{min} = \frac{DV_o}{V_r R_f}$$

Self-inductance and mutual inductance are calculated as

$$L_m = \beta L \text{ and } L_s = (1-\beta)L$$

$$\text{where } L = \frac{1 + \beta \frac{D}{1-D}}{1 + \beta - 2\beta^2} L_{eq}$$

VII SIMULATION MODEL AND RESULTS

SPV Panel (SOLKAR Panel- Model No. 3712/0507) $I_{scn} = 2.55A$; $V_{ocn} = 21.24 V$; $I_{mp} = 2.25A$; $V_{mp} = 16.56 V$;
 $P_{mp} = 37.08W$.

Converter $C_{in}=100\ \mu\text{F}$; $C_{out}=100\ \mu\text{F}$; $L=200\ \mu\text{H}$; $L_{m1}=9.7\text{mH}$; $L_{m2}=9.7\ \text{mH}$; $R_{load}=100$; $\beta=0.65$. Simulation results for $G=1000\ \text{W}/\text{m}^2$ and $T=25\ ^\circ\text{C}$ are presented.

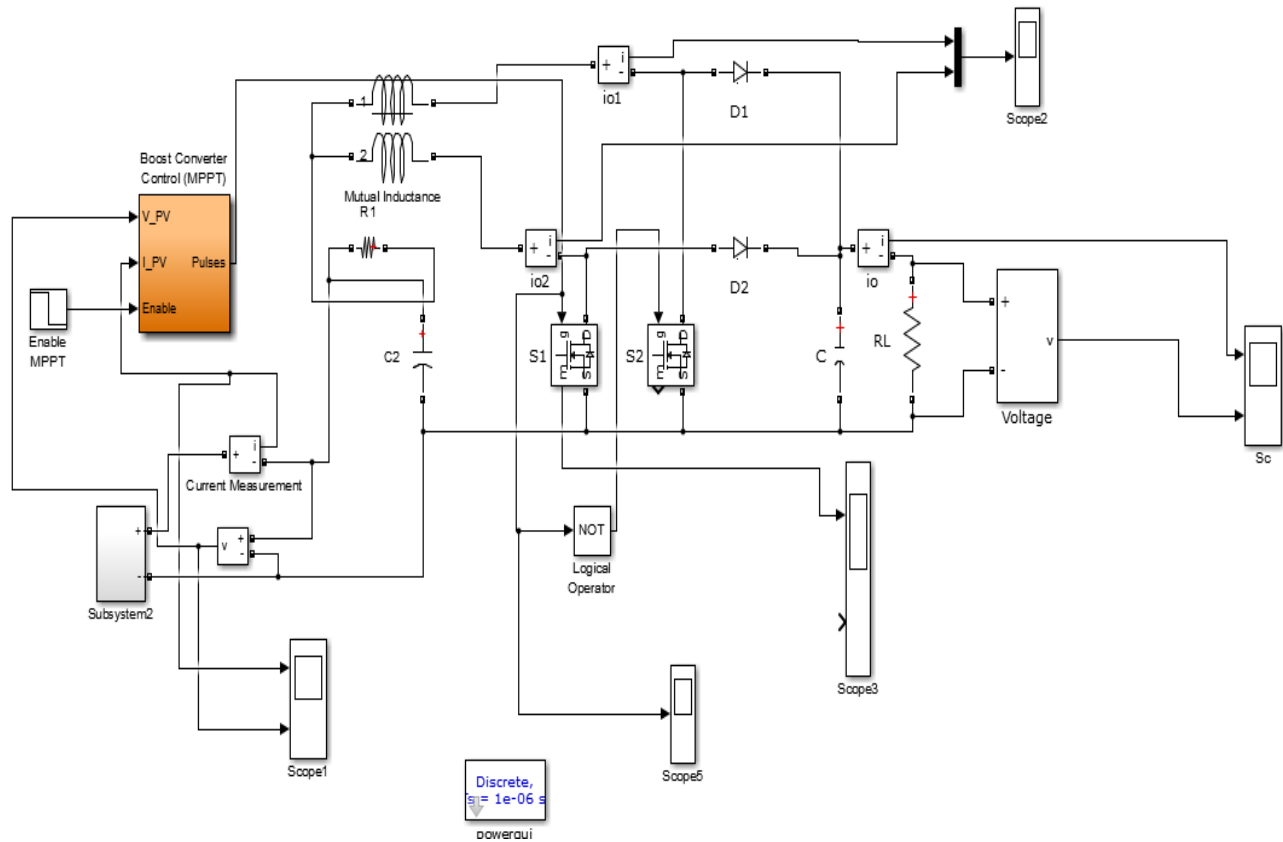
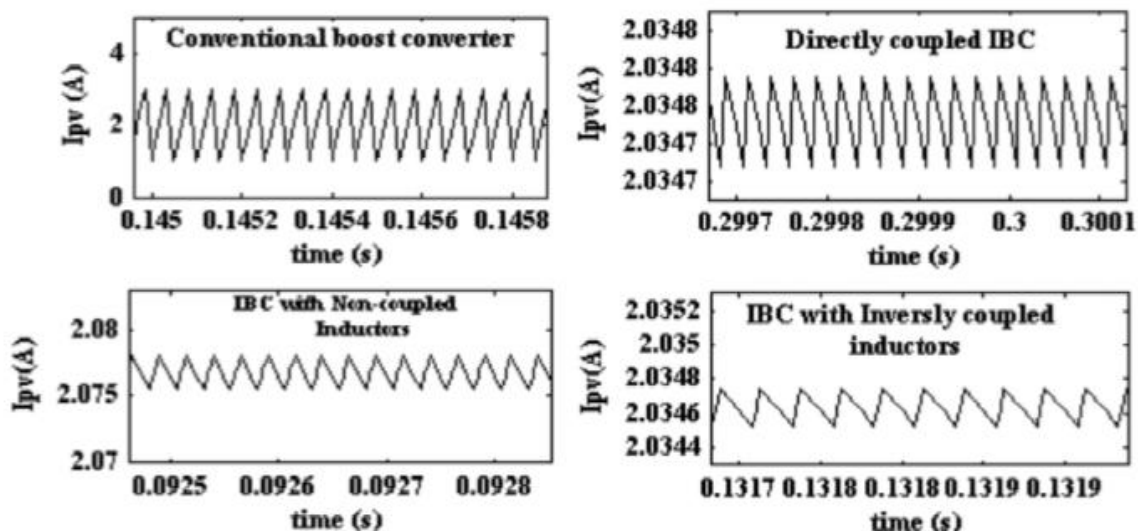
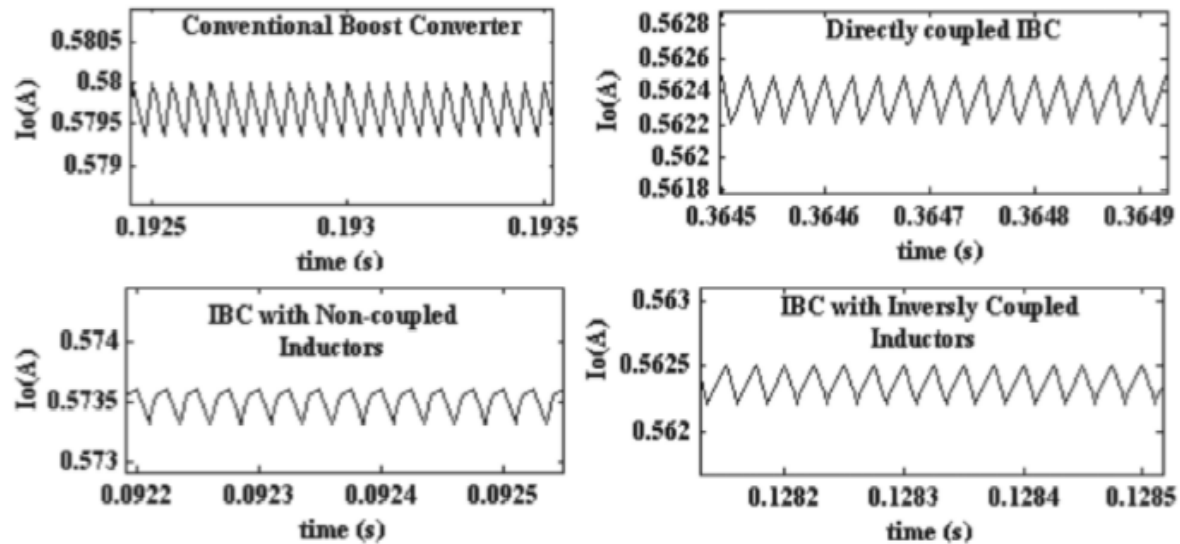


Fig.3 MATLAB modeling of IBC with PV input



Comparison of input current ripple



Comparison of output current ripple

VIII CONCLUSIONS

In this paper, a comparative analysis of the performance of conventional boost converters and different types of IBC interfaced with the SPV panel has been carried out. The parameter chosen for the analysis was the percentage ripple in the input and output currents, and output voltage. From the simulation results, it was found that IBC with directly coupled inductors reduced the ripple to a greater extent as compared to that of the other boost converter topologies. Hence, the value of the filter capacitor used was reduced.

REFERENCES

- [1] S.M. Chen, T.J. Liang, L.S. Yang, and J.F. Chen, A safety enhanced, high step-up dc-dc converter for ac photovoltaic module application. *IEEE Transactions on Power Electronics* 27, 2015, 1809–1817.
- [2] Y. Chen, H. Chen, Y. Chen, and K.H. Liu, A Stepping On-Time Adjustment Method for Interleaved Multichannel PFC Converters, *IEEE Transactions on Power Applications* 151, 2015, 1170–1176.
- [3] D. Zhang, Interleaved Boost Converter with Ripple Cancellation Network. *IEEE Transactions on Power Electronics*, 2012, 852–856
- [4] G.A.L. Henn, R.N.A.L. Silva, P.P. Praca, L.H.S.C. Barreto, and D.S. Oliveira, Interleaved-Boost Converter with High Voltage Gain, *IEEE Transactions on Power Applications* 25, 2010, 2753–2761.
- [5] B. Axelrod, Y. Berkovich, and A. Ioinovici, Switched-capacitor/switched-inductor structures for getting transformer less hybrid DC-DC PWM converters. *IEEE Transactions on Circuits System*, 55, 2008, 687–696.

5th International Conference on Science, Technology and Management

India International Centre, New Delhi

(ICSTM-16)

30th July 2016, www.conferenceworld.in

ISBN: 978-93-86171-00-9

- [6] Q. Li, and P. Wolfs, An analysis of the ZVS two-inductor boost converter under variable frequency operation. *IEEE Transactions on Power Electronics* 22, 2007, 120-131.
- [7] W. Li, and X. He, An interleaved winding-coupled boost converter with passive lossless clamp circuits. *IEEE Transactions on Power Electronics* 22, 2007, 1499-1507.
- [8] Y. Jang, and M.M. Jovanović, Interleaved boost converter with intrinsic voltage doubler characteristic for universal-line PFC front end. *IEEE Transactions on Power Electronics* 22, 2007, 1394–1401.
- [9] G.R. Walker, and P.C. Sernia, Cascaded DC–DC converter connection of photovoltaic modules. *IEEE Transactions on Power Electronics* 19, 2004, 1130–1139.
- [10] P.W. Lee, Y.S. Lee, D.K. Cheng, and X.C. Liu, Steady-state analysis of an interleaved boost converter with coupled inductors. *IEEE Transactions on Industrial Electronics* 47, 2000, 787-795.